Macromolecules

Article

Cite This: Macromolecules 2019, 52, 9291−9298

pubs.acs.org/Macromolecules

Shape Memory Behavior of Emulsion-Templated Poly(ε-Caprolactone) Synthesized by Organocatalyzed Ring-Opening Polymerization

Petra Utroša, Ozgun Can Onder, Ema Žagar, Sebastijan Kovačič,* and David Pahovnik*

Department of Polymer Chemistry and Technology, National Institute of Chemistry, Hajdrihova 19, 1000 Ljubljana, Slovenia

Supporting Information

ABSTRACT: Organocatalyzed ring-opening polymerization (ROP) of ε-caprolactone (CL) and 4,4′-bioxepanyl-7,7′-dione as a bis-lactone cross-linker was performed within the oil-in-oil high internal phase emulsions (HIPEs) at 50 °C. In this way, the cross-linked poly(ε-caprolactone) (PCL) polyHIPE foams of ∼85% porosity were synthesized. Thermomechanical properties of the prepared polyHIPEs were studied and proved to greatly depend on a degree of PCL cross-linking. The melting and crystallization temperatures as well as the degree of crystallinity of PCL polyHIPE foams decrease with an increasing cross-linking degree. Semi-crystalline polyHIPEs demonstrate shape memory behavior with excellent shape fixity and shape recovery. At an appropriate degree of PCL cross-linking, the polyHIPE temporary shape can be fixed at room temperature, while a transition to the permanent shape occurs upon heating at 40 °C. Moreover, a two-way shape memory behavior of the PCL polyHIPEs under constant stress was observed.

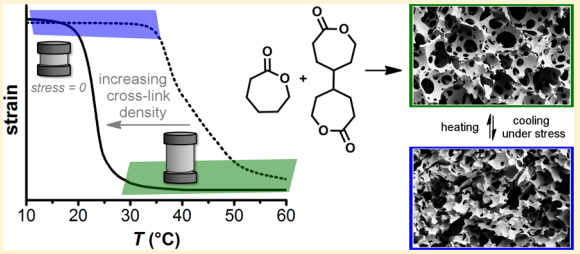

INTRODUCTION

High internal phase emulsion (HIPE) templating offers a route to produce highly interconnected porous polymer foams. Polymerized HIPEs (polyHIPEs) are typically prepared via free-radical polymerization of vinyl monomers in aqueous emulsions.[1,2] Lately, polyHIPE synthesis has been extended to other polymerization mechanisms, such as controlled radical polymerizations,[3,4] ring-opening metathesis polymerization (ROMP),[5,6] chain-growth insertion polymerization,[7] transition metal-catalyzed cross-couplings,[8] ring-opening polymerization (ROP),[9−11] and step-growth polymerizations (thiol-ene[12] and thiol-yne[13]). HIPE templating produces highly interconnected porous structures, especially suitable for tissue engineering scaffolds.[1] Degradable polyHIPEs based on poly(ε-caprolactone) (PCL) were synthesized, as PCL is an attractive and promising material for biomedical applications due to its good biocompatibility, degradability, and control over mechanical properties.[14,15] Furthermore, PCL is a semi-crystalline polymer and as such can exhibit shape memory behavior. The crystalline switching segments actuate a temporary shape when cycled through the transition (melting) temperature, whereas the cross-links establish and recover the permanent shape.[16,17] So far, bulk PCL-based materials have been extensively studied for their shape memory properties.[18−23] On the other hand, porous shape memory polymers can achieve higher deformations than bulk polymers and have lately become particularly interesting in biomedical applications, such as embolic vascular devices, drug-delivery platforms, and tissue scaffolds.[24,25] In compressed shape, they can be implanted into a human body through minimally invasive procedures, while by increasing the temperature at the implantation area, they can expand to fit into irregular shape defects.[26] So far, the shape memory phenomenon of polyHIPEs was reported only for the (meth)acrylate-based polyHIPEs, bearing the crystalline long side chains,[27,28] and for the polyHIPEs based on acrylamide and sodium acrylate that are capable of reversible metal coordination cross-linking.[29]

Hitherto, most PCL-based polyHIPEs have been prepared from the nonreactive high molecular weight PCL in water-in-oil emulsions via solvent evaporation[30−33] or by (co)-polymerization and simultaneous cross-linking of end-functionalized PCL macromonomers.[34−40] In all cases, PCL was dissolved/diluted to enable sufficient stirring of the system consisting of a highly viscous oil phase. For example, acrylic comonomers were used as the diluents for diacrylate-terminated PCL; however, an upper limit of PCL that could be incorporated into the polyHIPE during copolymerization was only 40−50 wt %.[34−36] Using toluene as a solvent instead of acrylic comonomer resulted in polyHIPEs with closed-cell morphology.[34] Open porosity of polyHIPEs was achieved by reacting PCL triol and diisocyanate diluted in toluene[37] or tetrahydrofuran (THF)[38] solvent; however, the PCL content in the obtained polyHIPEs was still around 50 wt % only. PolyHIPEs consisting of 76 wt % of PCL were obtained by thiol-ene reaction of triacrylate-terminated PCL with trithiol, where the presence of solvent was again essential for HIPE

Received: August 23, 2019
Revised: October 25, 2019
Published: November 26, 2019

formation.[39] Optimization of HIPE composition in terms of oil-phase dilution was also crucial for the preparation of pure PCL polyHIPEs from the four-arm PCL methacrylate macromonomer.[40] In an alternative procedure, liquid ε-caprolactone (CL) was used recently as a continuous phase of HIPE without the need to use a diluent.[10,11] Contrary to previous examples, the use of CL as a continuous phase requires oil-in-oil (O/O) HIPEs, since CL is miscible with water, which can additionally act as an initiator for ROP of CL. In this way, a noncross-linked polyHIPE based on PCL/poly(L-lactide) blend was prepared from an eutectic mixture of CL and L-lactide.[10] In another work, the cross-linked PCL-based polyHIPE was synthesized in O/O HIPE by ROP of CL and bis-lactone using stannous octoate as a catalyst at 120 °C.[11] At such a high polymerization temperature, a large amount of surfactant (37 wt %) has to be used to stabilize the O/O HIPE. Consequently, its complete removal from the final polyHIPE is difficult. Compared to aqueous emulsions, the O/O HIPEs are in general more difficult to stabilize. For this purpose, poly(ethylene glycol)-*block*-poly(propylene glycol)-*block*-poly(ethylene glycol) (PEG-*b*-PPG-*b*-PEG) triblock copolymers (Pluronics) have been reported as the efficient surfactants.[41] Commercial Pluronics contain terminal hydroxyl functional groups that can participate in ROP of CL as an initiator,[42] resulting in covalent incorporation of the surfactant into the polyHIPE structure.[43] Therefore, in this work, the hydroxyl groups of Pluronic F127 were methylated by iodomethane before its use as a surfactant for the preparation of PCL polyHIPEs.

Herein, a straightforward synthetic method for the preparation of cross-linked PCL-based polyHIPEs is reported. It takes full advantage of organocatalyzed ROP of cyclic esters that allows low temperature and rate controlled polymerization;[44,45] the parameters which are essential to control the HIPE stability until a well-defined polyHIPE structure is formed. The polyHIPEs were synthesized via the O/O HIPEs, where the liquid CL monomer along with the 4,4′-bioxepanyl-7,7′-dione (BOD) cross-linker, ethylene glycol initiator, diphenyl phosphate (DPP) catalyst, and modified surfactant served as a continuous phase, while petroleum benzine was used as an internal phase. The degree of PCL crystallinity and thus the thermomechanical properties of the as-obtained polyHIPEs were tuned by a degree of PCL cross-linking, which affected their thermally induced shape memory behavior.

EXPERIMENTAL SECTION

Chemicals. Chemicals: acetic acid (glacial, 100%, Merck), 4,4′-bicyclohexanone (98.0%, TCI), calcium hydride (95%, Sigma-Aldrich), DPP (99%, Aldrich), ethylene glycol (anhydrous, 99.8%, Sigma-Aldrich), formic acid (98%, Honeywell), iodomethane (99.5%, Sigma-Aldrich), magnesium sulfate (anhydrous, 99.5%, Sigma-Aldrich), Pluronic F127 (Sigma), sodium bicarbonate (Merck), sodium chloride (Fluka), sodium hydride (60% dispersion in mineral oil, Aldrich), sodium thiosulfate pentahydrate (Merck), and urea hydrogen peroxide (97%, Aldrich) and solvents: chloroform (Merck), 2-propanol (99.8%, Honeywell), ethanol (absolute, anhydrous, Carlo Erba), hexane (99%, Honeywell), petroleum benzine (boiling range 100−140 °C, Merck), and THF (anhydrous, 99.9%, Sigma-Aldrich) were used as received. CL (97%, Aldrich) was dried over calcium hydride and distilled under vacuum.

Methods. *^{1}H Nuclear Magnetic Resonance (NMR).* ^{1}H NMR spectra were recorded on a Varian Unity Inova 300 MHz instrument (Varian, Inc.). All measurements were carried out in $CDCl_3$ at room temperature in the pulse Fourier-transform mode. Tetramethylsilane (TMS, $\delta = 0$) was used as an internal chemical-shift standard. ^{1}H NMR data were processed using MestReNova software.

Fourier-Transform Infrared (FT-IR). FT-IR spectra were collected using a Spectrum One FT-IR spectrometer (Perkin Elmer, U.K.). FT-IR spectra were recorded in an attenuated total reflectance (ATR) mode in a spectral range of 650−4000 cm^{-1}.

Differential Scanning Calorimetry (DSC). DSC was used for investigation of thermal properties of polyHIPEs using a Mettler Toledo DSC 1 (Mettler Toledo, Switzerland). The samples were heated from −80 to 100 °C at a rate of 10 K min^{-1}, held at 100 °C for 1 min, then cooled to −80 °C at a rate of −2 K min^{-1}. After being held at −80 °C for 1 min, another heating to 100 °C at a rate of 10 K min^{-1} was performed. STARe software was used to determine transition temperatures and peak integrals. The results are given as an average of three measurements with standard deviation. The crystallinity of the sample (χ_c) was calculated using eq 1

$$\chi_c(\%) = 100 \times \frac{\Delta H_m}{\Delta H_m^0} \tag{1}$$

where ΔH_m was determined from the melting peak area. ΔH_m^0 of 100% crystalline PCL is 139.5 J g^{-1}.[46]

Scanning Electron Microscopy (SEM). SEM was used to investigate the morphology of polyHIPEs. Sample surfaces were sputtered with a 12 nm layer of gold using Q150T ES (Quorum Technologies, U.K.) prior scanning analysis. SEM images were taken on a Zeiss Supra 35 VP (Carl Zeiss, Germany). The pore size analysis of the SEM micrographs was performed by using Image J software. About 200 pores of each sample were measured, and, additionally, three samples of each polyHIPE type were analyzed.

Dynamic Mechanical Analysis (DMA). Mechanical tests were performed on a DMA Q800 (TA Instruments) dynamic thermal analyzer using the compression disks with 15 mm in diameter. Uniaxial compressive stress−strain measurements were conducted at different temperatures on the cylindrical specimens (∼7 mm diameter and ∼6 mm height) with force rate of 0.5 N min^{-1} up to 18 N. For a shape memory study, thermomechanical cycles were programmed as follows: a preload force of 0.005 N was applied and the temperature was equilibrated at 60 °C for polyHIPE-5.0 or 40 °C for polyHIPE-7.5 and held isothermally for 10 min. The sample's height was measured, and, afterward, the force was ramped with 0.3 and 0.6 N min^{-1} to 0.3 and 0.6 N for polyHIPE-5.0 and polyHIPE-7.5, respectively. The temperature was then decreased by 1 °C min^{-1} to 0 or 20 °C for polyHIPE-5.0, and −30 °C for polyHIPE-7.5, to allow sample crystallization. Then, the temperature was held isothermally for 20 min to obtain a temporary shape of the sample. The compressive load was then removed by −0.3 or −0.6 N min^{-1} to 0.005 N and again held isothermally for 20 min to assure the fixation. Afterward, the temperature was raised by 0.5 °C min^{-1} to 60 and 40 °C for polyHIPE-5.0 and polyHIPE-7.5, respectively, to determine the transition temperature and after that held isothermally for 60 min to regain the permanent shape of the samples. Cycles were repeated 1−6 times starting with the force ramp.

Shape fixity (R_f) and shape recovery (R_r) were calculated using eq 2 and 3

$$R_f\ (\%) = 100 \times \frac{\varepsilon_2}{\varepsilon_1} \tag{2}$$

$$R_r\ (\%) = 100 \times \frac{\varepsilon_1 - \varepsilon_3(N)}{\varepsilon_1 - \varepsilon_3(N-1)} \tag{3}$$

where ε_1 is the strain of the sample under load after cooling, ε_2 is the strain of the cooled sample after the load had been removed, and $\varepsilon_3(N)$ and $\varepsilon_3(N-1)$ are the final strains of the recovered samples above the T_m in two successive cycles (for $N = 1$, $\varepsilon_3(0)$ equals 0). For total recovery, $\varepsilon_3(N-1)$ is considered 0. The results are given as an average of three measurements with standard deviation.

Synthesis of BOD. BOD was prepared using an adapted procedure from the literature.[47] Urea hydrogen peroxide (20 g, 0.21 mol) and formic acid (100 mL) were stirred at room temperature for

DOI: 10.1021/acs.macromol.9b01780
Macromolecules 2019, 52, 9291−9298

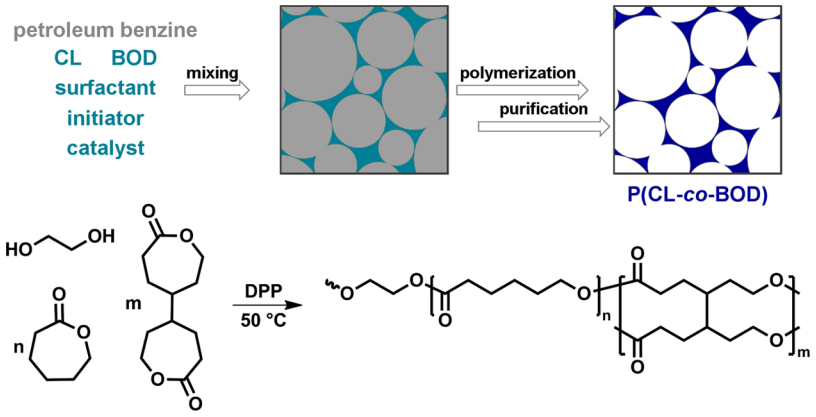

Figure 1. ROP of CL monomer and BOD cross-linker was conducted with ethylene glycol as an initiator and DPP as a catalyst. All reactants along with modified Pluronic surfactant were dissolved in CL, which served as the continuous phase of HIPE, while petroleum benzine served as an internal phase.

2 h. The reaction mixture was then cooled on ice, and bicyclohexanone (10 g, 0.05 mol) was slowly added. The mixture was stirred for further 4 h as the temperature reached the room temperature. Water (200 mL) was then added and the product was extracted with chloroform (1 × 200 mL, then 4 × 40 mL). Organic fractions were collected, washed with saturated aqueous sodium bicarbonate solution (4 × 150 mL) and brine (1 M, 200 mL), dried with anhydrous magnesium sulfate, and filtered. The solution was concentrated under reduced pressure and passed through the silica gel plug, using chloroform as an eluent. Finally, chloroform was evaporated under reduced pressure, and a white powder was obtained (66% yield). ^{1}H NMR ($CDCl_3$, 300 MHz, δ ppm): 4.38−4.12 (m, 2H, $-CH_2-O-$), 2.78−2.55 (m, 2H, $-CH_2-CO-$), 1.98−1.79 (m, 2H, $-O-CH_2-CH_2-$), 1.74−1.41 (m, 3H, $-CH-CH_2-$).

Surfactant Modification. PEG-*b*-PPG-*b*-PEG Pluronic F127 (10 g, 0.8 mmol) and sodium hydride (0.63 g of 60% oil dispersion, 15.9 mmol) were suspended in 30 mL of THF. The reaction mixture was cooled on ice and iodomethane was added (0.74 mL, 15.9 mmol). The reaction proceeded at room temperature for 48 h. Afterward, it was cooled on ice again and quenched with 2-propanol (30 mL), ethanol (2 mL), and acetic acid (until neutral pH). At this step, the color turned from transparent to orange. Solvents were removed on a rotary evaporator. To ensure complete solvent removal, the residue was dissolved in THF (75 mL) and evaporated again. Extraction of the product was performed as follows: the dry mixture was dissolved in chloroform (60 mL) and mixed twice with aqueous solution of sodium thiosulfate (5 wt %, 100 mL and 50 mL) until discoloration that indicated complete iodine reduction. The organic phase was washed with water (100 mL), dried with anhydrous magnesium sulfate, and filtered. Chloroform was evaporated to ∼10 mL. The product was then precipitated in hexane (250 mL) at −20 °C, centrifuged, washed twice with hexane (4 mL), and dried under vacuum overnight. The product is a white powder (89% yield). ^{1}H NMR ($CDCl_3$, 300 MHz): 3.72−3.60 (m, $-CH_2-CH_2-O-$), 3.60−3.46 (m, $-CH-CH_2-O-$), 3.46−3.30 (m, $-CH-CH_2-O-$), 3.38 (s, $-O-CH_3-$), 1.18−1.08 (m, $-CH-CH_3$).

PolyHIPE Preparation. A typical procedure for a polyHIPE with 90 vol % of internal phase and 5.0 mol % of BOD is as follows. BOD (0.16 g, 0.7 mmol) and modified F127 (0.34 g, 0.02 mmol) were dissolved in CL (1.5 mL, 13.5 mmol), followed by the addition of ethylene glycol (18.1 μL) and DPP (0.05 g, 0.2 mmol). Petroleum benzine (13.5 mL) was added dropwise while mixing on an overhead stirrer. After all of the internal phase had been added, the emulsion was mixed for another 10 min. The HIPE was then transferred to a plastic 2 mL Eppendorf tube, and polymerized at 50 °C overnight. The obtained polyHIPEs were washed on a Soxhlet extractor with diethyl ether for 24 h first to remove petroleum benzine as well as DPP to prevent any further unwanted transesterification reaction. Afterwards, washing was continued by ethanol for 24 h to remove the surfactant. Ethanol was then exchanged with deionized water by diffusion. Samples were finally freeze-dried to avoid shrinkage during drying. To verify the purity, extraction of polyHIPE with $CDCl_3$ (1800 μL) was performed on a dried and ground sample (14 mg). Gel fraction of the polyHIPE was determined using eq 4

$$\text{gel fraction (\%)} = 100 \times \frac{m_{\text{polyHIPE}} \times m_{(\text{EG+CL+BOD+DPP+surf.+PB})}}{m_{\text{HIPE}} \times m_{(\text{EG+CL+BOD})}} \quad (4)$$

where m_{HIPE} is mass of the sample before polymerization, m_{polyHIPE} is mass of the sample after polymerization and Soxhlet extraction, $m_{(\text{EG+CL+BOD})}$ is the total mass of ethylene glycol, CL, and BOD used for the preparation of the HIPE, and $m_{(\text{EG+CL+BOD+DPP+surf.+PB})}$ is the total mass of ethylene glycol, CL, BOD, DPP, surfactant, and petroleum benzine used for the preparation of the HIPE. The results are given as an average of three measurements with standard deviation.

RESULTS AND DISCUSSION

For the preparation of stable HIPEs with 90 vol % of the internal phase, 16 wt % of the surfactant in the continuous phase was needed. DPP was used as an organocatalyst since it offers a high degree of control over ROP of CL in solution,[48] as well as in bulk.[49] Since ROP of CL proceeds at room temperature already, a proper amount of added catalyst is of utmost importance. Its concentration should be high enough to induce gelation of the system within the HIPE stability period, while on the other hand, the catalyst concentration should be low enough to keep the emulsion viscosity at the levels suitable for mechanical stirring. In both respects, 3 wt % of DPP was found to be an optimum added amount. After curing the HIPEs for 16 h at 50 °C (Figure 1), a complete consumption of the monomer and cross-linker was confirmed by ^{1}H NMR of the $CDCl_3$ extracts of the obtained nonpurified polyHIPEs (Figure S4).

PCL polyHIPE samples were prepared with 5.0 and 7.5 mol % of BOD cross-linker, and so the samples are denoted as polyHIPE-5.0 and polyHIPE-7.5, respectively. Gel fractions of the polyHIPEs after purification were above 85% (Table 1), indicating highly cross-linking materials. Higher gel fraction determined for the polyHIPE-7.5 is ascribed to a higher amount of the cross-linker used. Densities of the samples were measured and used to calculate the polyHIPEs' porosity (Table 1). The porosity of both samples was comparable,

DOI: 10.1021/acs.macromol.9b01780
Macromolecules 2019, 52, 9291−9298

which was expected since the volume fraction of the internal phase was the same for both samples. The cross-section images of the monoliths (Figure 2) reveal typical polyHIPE morphology, with an average void size of around 30 μm for both samples.

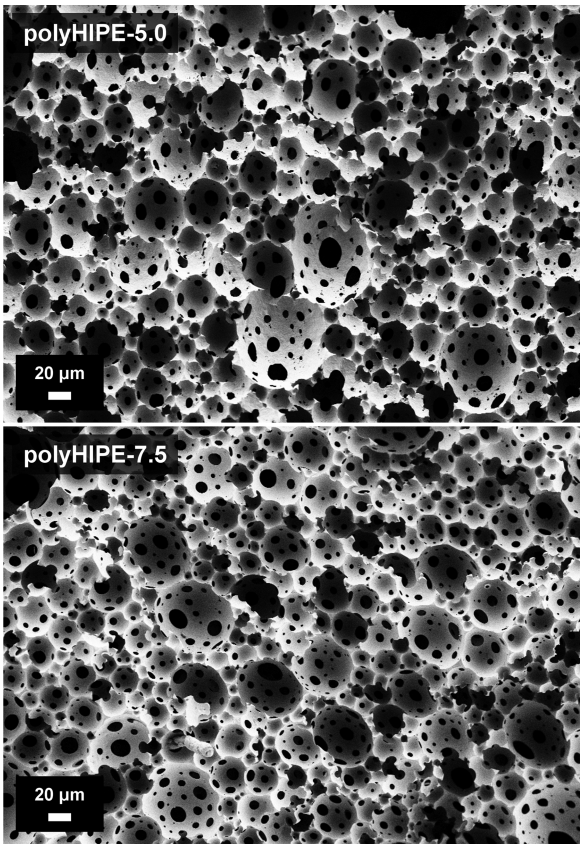

Figure 2. SEM micrographs of polyHIPE-5.0 and polyHIPE-7.5 showing typical polyHIPE morphology with voids and interconnecting windows.

The degree of crystallinity (χ_c), melting temperature (T_m), and crystallization temperature (T_c) of PCL-based polyHIPEs were determined by DSC (Table 1 and Figure 3). The values of T_m, T_c, and χ_c decrease with an increasing amount of BOD cross-linker, since randomly distributed cross-links along the PCL chains disrupt PCL crystallization.[50] Cross-linking density affects the thermal properties of polyHIPE materials (polyHIPE-5.0 crystallizes at 3.7 °C and melts at 32.4 °C, while polyHIPE-7.5 has a T_c of −19.0 °C and T_m of 18.4 °C), which is further reflected in their mechanical properties.

The compressive stress−strain curves and Young's moduli (E) measured at −30, 20, and 60 °C are presented in Figure 4A,B. The moduli of polyHIPEs significantly decrease with

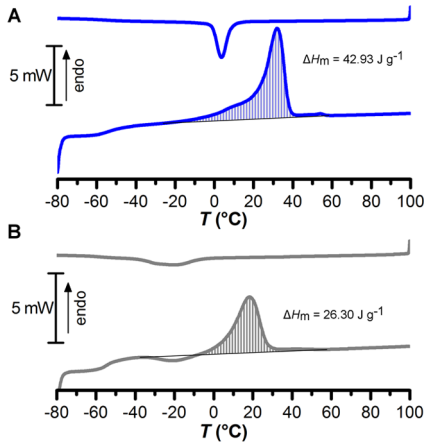

Figure 3. DSC thermograms of polyHIPE-5.0 (A) and polyHIPE-7.5 (B). First cooling (−2 K min^{-1}) and second heating (10 K min^{-1}) with melting enthalpy (ΔH_m) are represented.

increasing temperature and cross-linker amount. At 20 °C, polyHIPE-5.0 shows an initial linear elastic region in the stress−strain curve. Further increase in stress causes wall buckling, as can be observed in Figure 4C, which is reflected in a plateau of the stress−strain curve. Afterward, a sharp increase in the stress is observed most likely due to the densification of the material.[25,51] By increasing the temperature, PCL starts to soften due to melting, and hence it becomes more easily deformed. Nevertheless, the PCL network, unlike linear PCL, keeps its mechanical integrity due to the presence of chemical cross-links. This allows the shaping of the cross-linked material above its melting point to induce the imposed, temporary shape of the polyHIPE. The softened sample was compressed to a half of its original height and left to cool down below its crystallization temperature, upon which the PCL crystalline domains reformed, and thus lock a new shape of the polyHIPE. When the compressive load was removed, the imposed temporary shape was obtained where the voids in the polyHIPE are highly compacted and difficult to distinguish, as indicated by SEM micrographs in Figure 4C. By increasing the temperature above the T_m again, the crystalline domains melt and the network regains its initial, permanent shape with fully recovered polyHIPE void morphology (Figures 4D and S5), thus demonstrating the shape memory behavior of the PCL polyHIPE materials.

Shape memory behavior was quantitatively studied by cyclic thermomechanical compression testing. The material's shape memory performance depends on a degree of deformation that is exerted upon the melted sample. Increasing the compressive force on the polyHIPE-5.0 causes higher strain as well as better shape fixation, while the shape recovery slightly decreases (Figures S6 and S7). Therefore, the shape memory cycles began by compressing the melted polyHIPE to ∼50% (Figures

Table 1. Structural and Thermal Properties of PCL-Based PolyHIPEs

sample	gel fraction[a] wt %	density[b] g cm^{-3}	calc. porosity[c] %	average pore size[d] μm	χ_c[e] %	T_m °C	T_c °C
polyHIPE-5.0	91.1 ± 5.2	0.17 ± 0.01	85.1 ± 0.7	32.6 ± 13.0	30.2 ± 0.6	32.4 ± 0.2	3.7 ± 1.3
polyHIPE-7.5	97.0 ± 2.8	0.18 ± 0.01	83.9 ± 0.4	28.9 ± 14.0	18.9 ± 0.3	18.4 ± 0.1	−19.0 ± 1.2

[a]Monolith mass after Soxhlet extraction. [b]Density determined by mass and geometry of dry monolith. [c]Calculated based on the density of bulk cross-linked PCL (1.15 g cm^{-3}). [d]Determined from SEM micrographs by measuring ∼200 pores of one sample, while deviation among the measurements of three parallel samples was found to be ∼15%. [e]Calculated from melting enthalpy in DSC thermogram of PCL polyHIPE and taking into account the melting enthalpy of 100% crystalline PCL.

DOI: 10.1021/acs.macromol.9b01780
Macromolecules 2019, 52, 9291−9298

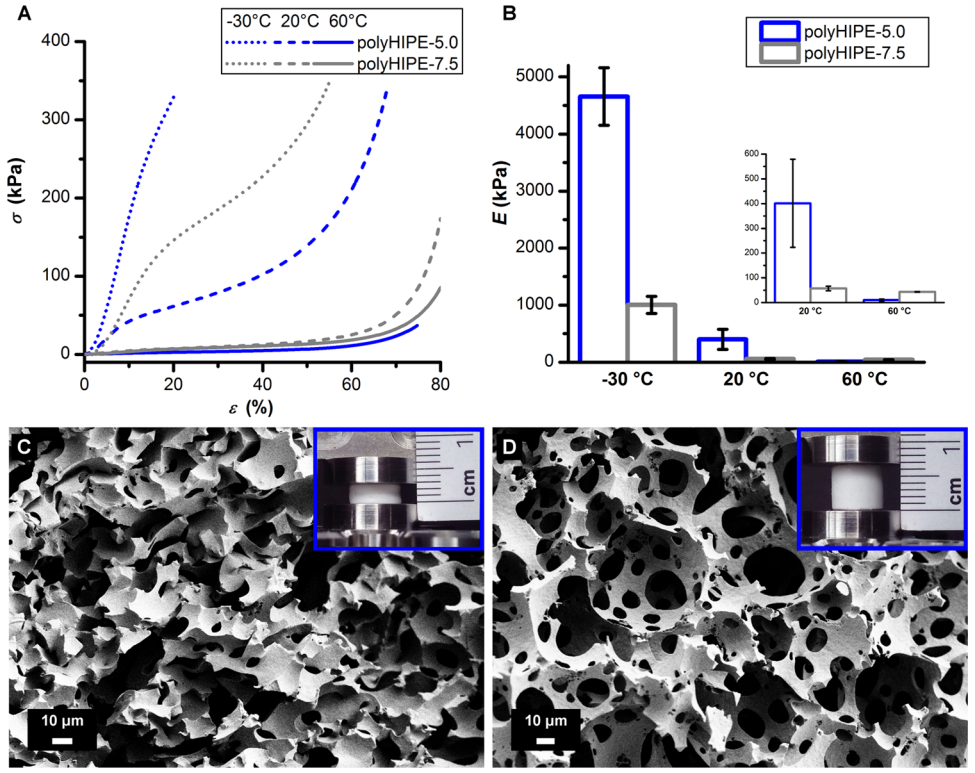

Figure 4. Compressive stress−strain (σ vs ε) curves of polyHIPE-5.0 and polyHIPE-7.5 measured at different temperatures (A). Young's moduli (E) determined from a slope of the initial linear region of the compressive stress−strain curve (B). SEM micrographs of polyHIPE-5.0 fixed shape when compressed to ∼50% strain at 20 °C (C) and the following recovered shape after being heated to 60 °C (D).

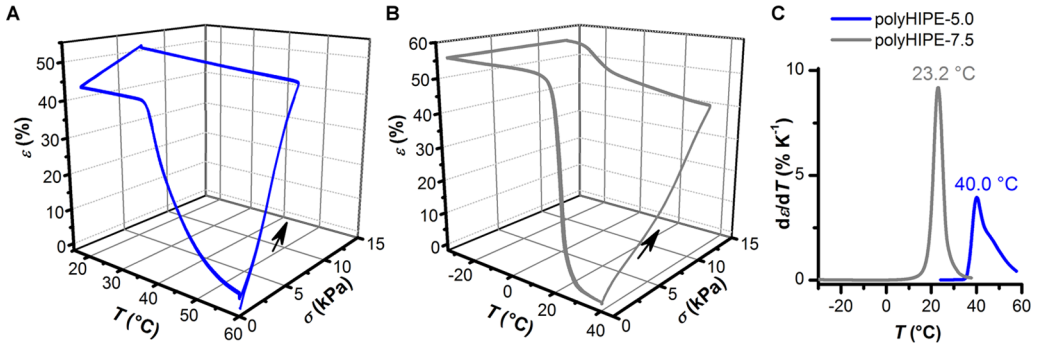

Figure 5. Stress (σ), strain (ε), and temperature (T) for four consecutive shape memory cycles for polyHIPE-5.0 (A) and polyHIPE-7.5 (B). Arrows indicate the beginning and direction of the process. Temperature derivative of strain ($d\varepsilon/dT$) during the recovery process of the first shape memory cycle (C).

Table 2. Shape Fixity Ratio (R_f) and Shape Recovery Ratio (R_r) of Consecutive Shape Memory Cycles for PolyHIPE-5.0 (Shape Fixed at 20 °C and Recovered at 60 °C) and PolyHIPE-7.5 (Shape Fixed at −30 °C and Recovered at 40 °C)

sample		1	2	3	4	5	6
polyHIPE-5.0	R_f	84.8 ± 6.2	84.6 ± 6.3	84.5 ± 6.3	84.3 ± 6.5	84.3 ± 6.3	84.4 ± 6.4
	R_r	90.5 ± 10.5	99.5 ± 0.5	99.7 ± 0.3	99.9 ± 0.4	100.2 ± 0.8	99.8 ± 0.1
polyHIPE-7.5	R_f	99.8 ± 0.1	99.7 ± 0.1	99.8 ± 0.1	99.7 ± 0.1		
	R_r	99.4 ± 0.4	99.9 ± 0.1	99.9 ± 0.1	100.1 ± 0.1		

5 and S8). Upon slowly cooling the polyHIPE below the T_c to fix the imposed temporary shape, some additional deformation was observed, which could be attributed to creep, thermal contraction, and/or ordered crystallization of the PCL chains.[52,53] The load was then removed and the percentage of the retained temporary shape was quantified by the shape fixity (R_f) (Table 2), which depends on fixing temperature. When the material was fixed at the temperature below its crystallization region (i.e., polyHIPE-7.5 at −30 °C and polyHIPE-5.0 at 0 °C), the fixation is above 99%. However, polyHIPE-5.0 still reaches the R_f of 84% when cooled at 20 °C, where it is partially melted. This proves the stability of the imposed temporary shape of the polyHIPE-5.0 at room temperature. Next, by increasing the temperature above the

DOI: 10.1021/acs.macromol.9b01780
Macromolecules 2019, 52, 9291−9298

T_m again, the permanent shape is regained and quantified by the shape recovery ratio (R_r) (Table 2). The R_r values of the first shape memory cycle are somewhat lower, which is known as the so-called training phenomenon.[18] Nevertheless, the proceeding cycles are characterized by excellent R_r, which is higher than 99%. The transition temperature (T_{trans}) at which the shape recovery occurs was determined by the steepest increase in strain during slow heating, which was evaluated by a maximum of the strain derivative (Figure 5C). The T_{trans} of the polyHIPE-5.0 is 40.0 °C and differs significantly from that of the polyHIPE-7.5, which exhibits T_{trans} at 23.2 °C. T_{trans} is in agreement with the T_m as determined by DSC, taking into account the broad melting peaks.

Deformation of synthesized polyHIPEs observed upon cooling was further investigated by conducting the thermomechanical cycles under constant stress. During crystallization under minimal stress, only ∼3% of compressive strain was observed, which can be ascribed to the thermal contraction as a consequence of crystallization. However, cooling the polyHIPEs after being compressed to ∼50% caused a significant additional strain (Figure S9). After crystallization, the samples were reheated under stress. The additional compressive strain was recovered, indicating that stress, besides temperature, induced crystallization of PCL chains into more ordered structures. These results thus reveal the so-called two-way shape memory behavior of our polyHIPEs, since the material is able to vary between the shapes upon temperature change only. Such behavior was more pronounced for the polyHIPE-7.5 with a higher degree of cross-linking, most probably due to its slower crystallization and, consequently, longer time required for the PCL chains to form ordered crystalline structures that act as physical cross-links.[52]

CONCLUSIONS

In this work, a straightforward synthetic method for the preparation of well-defined PCL-based polyHIPEs by using organocatalyzed ROP of CL within the HIPE is established. The obtained PCL polyHIPE foams demonstrate shape memory behavior with excellent fixity and recovery ratios and clear effects of cross-linking degree on their thermomechanical properties. PCL polyHIPEs as presented herein may find an interest as the scaffolds for biomedical applications, and the described method for the preparation of cross-linked polyHIPEs may be extended to other cyclic monomers that are able to polymerize by ROP.

ASSOCIATED CONTENT

Supporting Information

The Supporting Information is available free of charge at https://pubs.acs.org/doi/10.1021/acs.macromol.9b01780.

^{1}H NMR spectra; FT-IR spectrum; SEM micrograph; and shape memory study (PDF)

AUTHOR INFORMATION

Corresponding Authors

*E-mail: sebastijan.kovacic@ki.si (S.K.).
*E-mail: david.pahovnik@ki.si (D.P.).

ORCID

Ozgun Can Onder: 0000-0003-1878-1215
Ema Žagar: 0000-0002-2694-4312
Sebastijan Kovačič: 0000-0003-2664-9791
David Pahovnik: 0000-0001-8024-8871

Notes

The authors declare no competing financial interest.

ACKNOWLEDGMENTS

The authors acknowledge the financial support from the Slovenian Research Agency (Research Core Funding No. P2-0145 and project No. J2-9214). P.U. is a Ph.D. student at the Faculty of Chemistry and Chemical Engineering, University of Maribor, Slovenia.

REFERENCES

(1) Silverstein, M. S. PolyHIPEs: Recent Advances in Emulsion-Templated Porous Polymers. *Prog. Polym. Sci.* **2014**, *39*, 199−234.
(2) Cameron, N. R. High Internal Phase Emulsion Templating as a Route to Well-Defined Porous Polymers. *Polymer* **2005**, *46*, 1439−1449.
(3) Cummins, D.; Wyman, P.; Duxbury, C. J.; Thies, J.; Koning, C. E.; Heise, A. Synthesis of Functional Photopolymerized Macroporous PolyHIPEs by Atom Transfer Radical Polymerization Surface Grafting. *Chem. Mater.* **2007**, *19*, 5285−5292.
(4) Luo, Y.; Wang, A.-N.; Gao, X. Pushing the Mechanical Strength of PolyHIPEs up to the Theoretical Limit through Living Radical Polymerization. *Soft Matter* **2012**, *8*, 1824−1830.
(5) Deleuze, H.; Faivre, R.; Herroguez, V. Preparation and Functionalisation of Emulsion-Derived Microcellular Polymeric Foams (PolyHIPEs) by Ring-Opening Metathesis Polymerisation (ROMP). *Chem. Commun.* **2002**, 2822−2823.
(6) Kovačič, S.; Krajnc, P.; Slugovc, C. Inherently Reactive PolyHIPE Material from Dicyclopentadiene. *Chem. Commun.* **2010**, *46*, 7504−7506.
(7) Slováková, E.; Ješelnik, M.; Žagar, E.; Zedník, J.; Sedláček, J.; Kovačič, S. Chain-Growth Insertion Polymerization of 1,3-Diethynylbenzene High Internal Phase Emulsions into Reactive π-Conjugated Foams. *Macromolecules* **2014**, *47*, 4864−4869.
(8) Zhang, K.; Vobecka, Z.; Tauer, K.; Antonietti, M.; Vilela, F. π-Conjugated PolyHIPEs as Highly Efficient and Reusable Heterogeneous Photosensitizers. *Chem. Commun.* **2013**, *49*, 11158−11160.
(9) Sharma, E.; Samanta, A.; Pal, J.; Bahga, S. S.; Nandan, B.; Srivastava, R. K. High Internal Phase Emulsion Ring-Opening Polymerization of Pentadecanolide: Strategy to Obtain Porous Scaffolds in a Single Step. *Macromol. Chem. Phys.* **2016**, *217*, 1752−1758.
(10) Pérez-García, M. G.; Gutiérrez, M. C.; Mota-Morales, J. D.; Luna-Bárcenas, G.; del Monte, F. Synthesis of Biodegradable Macroporous Poly(L-Lactide)/Poly(ε-Caprolactone) Blend Using Oil-in-Eutectic-Mixture High-Internal-Phase Emulsions as Template. *ACS Appl. Mater. Interfaces* **2016**, *8*, 16939−16949.
(11) Yadav, A.; Pal, J.; Nandan, B.; Srivastava, R. K. Macroporous Scaffolds of Cross-Linked Poly(ε-Caprolactone) via High Internal Phase Emulsion Templating. *Polymer* **2019**, *176*, 66−73.
(12) Sergent, B.; Birot, M.; Deleuze, H. Preparation of Thiol−Ene Porous Polymers by Emulsion Templating. *React. Funct. Polym.* **2012**, *72*, 962−966.
(13) Chen, C.; Eissa, A. M.; Schiller, T. L.; Cameron, N. R. Emulsion-Templated Porous Polymers Prepared by Thiol-Ene and Thiol-Yne Photopolymerisation Using Multifunctional Acrylate and Non-Acrylate Monomers. *Polymer* **2017**, *126*, 395−401.
(14) Albertsson, A.-C.; Varma, I. K. Recent Developments in Ring Opening Polymerization of Lactones for Biomedical Applications. *Biomacromolecules* **2003**, *4*, 1466−1486.
(15) Woodruff, M. A.; Hutmacher, D. W. The Return of a Forgotten Polymer—Polycaprolactone in the 21st Century. *Prog. Polym. Sci.* **2010**, *35*, 1217−1256.
(16) Lendlein, A.; Kelch, S. Shape-Memory Polymers. *Angew. Chem., Int. Ed.* **2002**, *41*, 2034−2057.

DOI: 10.1021/acs.macromol.9b01780
Macromolecules 2019, 52, 9291−9298

(17) Hager, M. D.; Bode, S.; Weber, C.; Schubert, U. S. Shape Memory Polymers: Past, Present and Future Developments. *Prog. Polym. Sci.* **2015**, *49*−*50*, 3−33.
(18) Defize, T.; Riva, R.; Raquez, J.-M.; Dubois, P.; Jérôme, C.; Alexandre, M. Thermoreversibly Crosslinked Poly(ε-Caprolactone) as Recyclable Shape-Memory Polymer Network. *Macromol. Rapid Commun.* **2011**, *32*, 1264−1269.
(19) Raquez, J.-M.; Vanderstappen, S.; Meyer, F.; Verge, P.; Alexandre, M.; Thomassin, J.-M.; Jérôme, C.; Dubois, P. Design of Cross-Linked Semicrystalline Poly(ε-Caprolactone)-Based Networks with One-Way and Two-Way Shape-Memory Properties through Diels-Alder Reactions. *Chem. − Eur. J.* **2011**, *17*, 10135−10143.
(20) Defize, T.; Riva, R.; Thomassin, J.-M.; Jérôme, C.; Alexandre, M. Thermo-Reversible Reactions for the Preparation of Smart Materials: Recyclable Covalently-Crosslinked Shape Memory Polymers. *Macromol. Symp.* **2011**, *309*−*310*, 154−161.
(21) Defize, T.; Riva, R.; Jérôme, C.; Alexandre, M. Multifunctional Poly(ε-Caprolactone)-Forming Networks by Diels-Alder Cycloaddition: Effect of the Adduct on the Shape-Memory Properties. *Macromol. Chem. Phys.* **2012**, *213*, 187−197.
(22) Defize, T.; Riva, R.; Thomassin, J.-M.; Alexandre, M.; Herck, N. V.; Prez, F. D.; Jérôme, C. Reversible TAD Chemistry as a Convenient Tool for the Design of (Re)Processable PCL-Based Shape-Memory Materials. *Macromol. Rapid Commun.* **2017**, *38*, No. 1600517.
(23) Defize, T.; Thomassin, J.-M.; Ottevaere, H.; Malherbe, C.; Eppe, G.; Jellali, R.; Alexandre, M.; Jérôme, C.; Riva, R. Photo-Cross-Linkable Coumarin-Based Poly(ε-Caprolactone) for Light-Controlled Design and Reconfiguration of Shape-Memory Polymer Networks. *Macromolecules* **2019**, *52*, 444−456.
(24) Hasan, S. M.; Nash, L. D.; Maitland, D. J. Porous Shape Memory Polymers: Design and Applications. *J. Polym. Sci., Part B: Polym. Phys.* **2016**, *54*, 1300−1318.
(25) Hearon, K.; Singhal, P.; Horn, J.; Small, W.; Olsovsky, C.; Maitland, K. C.; Wilson, T. S.; Maitland, D. J. Porous Shape-Memory Polymers. *Polym. Rev.* **2013**, *53*, 41−75.
(26) Zhang, D.; George, O. J.; Petersen, K. M.; Jimenez-Vergara, A. C.; Hahn, M. S.; Grunlan, M. A. A Bioactive "Self-Fitting" Shape Memory Polymer Scaffold with Potential to Treat Cranio-Maxillo Facial Bone Defects. *Acta Biomater.* **2014**, *10*, 4597−4605.
(27) Gurevitch, I.; Silverstein, M. S. Shape Memory Polymer Foams from Emulsion Templating. *Soft Matter* **2012**, *8*, 10378−10387.
(28) Warwar Damouny, C.; Silverstein, M. S. Hydrogel-Filled, Semi-Crystalline, Nanoparticle-Crosslinked, Porous Polymers from Emulsion Templating: Structure, Properties, and Shape Memory. *Polymer* **2016**, *82*, 262−273.
(29) Zhang, T.; Silverstein, M. S. Doubly-Crosslinked, Emulsion-Templated Hydrogels through Reversible Metal Coordination. *Polymer* **2017**, *126*, 386−394.
(30) Hu, Y.; Gao, H.; Du, Z.; Liu, Y.; Yang, Y.; Wang, C. Pickering High Internal Phase Emulsion-Based Hydroxyapatite−Poly(ε-Caprolactone) Nanocomposite Scaffolds. *J. Mater. Chem. B* **2015**, *3*, 3848−3857.
(31) Samanta, A.; Nandan, B.; Srivastava, R. K. Morphology of Electrospun Fibers Derived from High Internal Phase Emulsions. *J. Colloid Interface Sci.* **2016**, *471*, 29−36.
(32) Yang, T.; Hu, Y.; Wang, C.; Binks, B. P. Fabrication of Hierarchical Macroporous Biocompatible Scaffolds by Combining Pickering High Internal Phase Emulsion Templates with Three-Dimensional Printing. *ACS Appl. Mater. Interfaces* **2017**, *9*, 22950−22958.
(33) Hu, Y.; Wang, J.; Li, X.; Hu, X.; Zhou, W.; Dong, X.; Wang, C.; Yang, Z.; Binks, B. P. Facile Preparation of Bioactive Nanoparticle/Poly(ε-Caprolactone) Hierarchical Porous Scaffolds via 3D Printing of High Internal Phase Pickering Emulsions. *J. Colloid Interface Sci.* **2019**, *545*, 104−115.
(34) Busby, W.; Cameron, N. R.; Jahoda, C. A. B. Emulsion-Derived Foams (PolyHIPEs) Containing Poly(ε-Caprolactone) as Matrixes for Tissue Engineering. *Biomacromolecules* **2001**, *2*, 154−164.
(35) Lumelsky, Y.; Silverstein, M. S. Biodegradable Porous Polymers through Emulsion Templating. *Macromolecules* **2009**, *42*, 1627−1633.
(36) Lumelsky, Y.; Lalush-Michael, I.; Levenberg, S.; Silverstein, M. S. A Degradable, Porous, Emulsion-Templated Polyacrylate. *J. Polym. Sci., Part A: Polym. Chem.* **2009**, *47*, 7043−7053.
(37) Changotade, S.; Radu Bostan, G.; Consalus, A.; Poirier, F.; Peltzer, J.; Lataillade, J.-J.; Lutomski, D.; Rohman, G. Preliminary *In Vitro* Assessment of Stem Cell Compatibility with Cross-Linked Poly(ε-Caprolactone Urethane) Scaffolds Designed through High Internal Phase Emulsions. *Stem Cells Int.* **2015**, *2015*, No. 283796.
(38) David, D.; Silverstein, M. S. Porous Polyurethanes Synthesized within High Internal Phase Emulsions. *J. Polym. Sci., Part A: Polym. Chem.* **2009**, *47*, 5806−5814.
(39) Johnson, D. W.; Langford, C. R.; Didsbury, M. P.; Lipp, B.; Przyborski, S. A.; Cameron, N. R. Fully Biodegradable and Biocompatible Emulsion Templated Polymer Scaffolds by Thiol-Acrylate Polymerization of Polycaprolactone Macromonomers. *Polym. Chem.* **2015**, *6*, 7256−7263.
(40) Aldemir Dikici, B.; Sherborne, C.; Reilly, G. C.; Claeyssens, F. Emulsion Templated Scaffolds Manufactured from Photocurable Polycaprolactone. *Polymer* **2019**, *175*, 243−254.
(41) Cameron, N. R.; Sherrington, D. C. Non-Aqueous High Internal Phase Emulsions. Preparation and Stability. *J. Chem. Soc., Faraday Trans.* **1996**, *92*, 1543−1547.
(42) Zhao, J.; Gou, M.; Dai, M.; Li, X.; Cao, M.; Huang, M.; Wen, Y.; Kan, B.; Qian, Z.; Wei, Y. Preparation, Characterization, and *in Vitro* Cytotoxicity Study of Cationic PCL-Pluronic-PCL (PCFC) Nanoparticles for Gene Delivery. *J. Biomed. Mater. Res., Part A* **2009**, *90A*, 506−513.
(43) Kovačič, S.; Preishuber-Pflügl, F.; Pahovnik, D.; Žagar, E.; Slugovc, C. Covalent Incorporation of the Surfactant into High Internal Phase Emulsion Templated Polymeric Foams. *Chem. Commun.* **2015**, *51*, 7725−7728.
(44) Kamber, N. E.; Jeong, W.; Waymouth, R. M.; Pratt, R. C.; Lohmeijer, B. G. G.; Hedrick, J. L. Organocatalytic Ring-Opening Polymerization. *Chem. Rev.* **2007**, *107*, 5813−5840.
(45) Utroša, P.; Žagar, E.; Kovačič, S.; Pahovnik, D. Porous Polystyrene Monoliths Prepared from *in Situ* Simultaneous Interpenetrating Polymer Networks: Modulation of Morphology by Polymerization Kinetics. *Macromolecules* **2019**, *52*, 819−826.
(46) Crescenzi, V.; Manzini, G.; Calzolari, G.; Borri, C. Thermodynamics of Fusion of Poly-β-Propiolactone and Poly-ε-Caprolactone. Comparative Analysis of the Melting of Aliphatic Polylactone and Polyester Chains. *Eur. Polym. J.* **1972**, *8*, 449−463.
(47) Nguyen, N. T.; Thurecht, K. J.; Howdle, S. M.; Irvine, D. J. Facile One-Spot Synthesis of Highly Branched Polycaprolactone. *Polym. Chem.* **2014**, *5*, 2997−3008.
(48) Makiguchi, K.; Satoh, T.; Kakuchi, T. Diphenyl Phosphate as an Efficient Cationic Organocatalyst for Controlled/Living Ring-Opening Polymerization of δ-Valerolactone and ε-Caprolactone. *Macromolecules* **2011**, *44*, 1999−2005.
(49) Saito, T.; Aizawa, Y.; Tajima, K.; Isono, T.; Satoh, T. Organophosphate-Catalyzed Bulk Ring-Opening Polymerization as an Environmentally Benign Route Leading to Block Copolyesters, End-Functionalized Polyesters, and Polyester-Based Polyurethane. *Polym. Chem.* **2015**, *6*, 4374−4384.
(50) Pitt, C. G.; Hendren, R. W.; Schindler, A.; Woodward, S. C. The Enzymatic Surface Erosion of Aliphatic Polyesters. *J. Controlled Release* **1984**, *1*, 3−14.
(51) Onder, O. C.; Yilgor, E.; Yilgor, I. Preparation of Monolithic Polycaprolactone Foams with Controlled Morphology. *Polymer* **2018**, *136*, 166−178.
(52) Dolynchuk, O.; Kolesov, I.; Jehnichen, D.; Reuter, U.; Radusch, H.-J.; Sommer, J.-U. Reversible Shape-Memory Effect in Cross-Linked Linear Poly(ε-Caprolactone) under Stress and Stress-Free Conditions. *Macromolecules* **2017**, *50*, 3841−3854.
(53) Baker, R. M.; Henderson, J. H.; Mather, P. T. Shape Memory Poly(ε-Caprolactone)-*Co*-Poly(Ethylene Glycol) Foams with Body

DOI: 10.1021/acs.macromol.9b01780
Macromolecules 2019, 52, 9291−9298

Temperature Triggering and Two-Way Actuation. *J. Mater. Chem. B* **2013**, *1*, 4916−4920.

DOI: 10.1021/acs.macromol.9b01780
Macromolecules 2019, 52, 9291−9298